Cold Regions Science and Technology 158 (2019) 117–127

Contents lists available at ScienceDirect

Cold Regions Science and Technology

journal homepage: www.elsevier.com/locate/coldregions

Thermal modeling of heat balance through embankments in permafrost regions

Xiangbing Kong[a,*], Guy Doré[a], Fabrice Calmels[b]

[a] Department of Civil and Water Engineering, Laval University, Québec City, Québec, Canada
[b] Yukon Research Centre/Northern Climate ExChange, Yukon College, Whitehorse, Yukon, Canada

ARTICLE INFO

Keywords:
Permafrost degradation
Transportation infrastructure
Alaska highway
Thermal modeling
Heat balance

ABSTRACT

Permafrost is widely distributed in the northern hemisphere and permafrost degradation underneath transportation infrastructure is on-going due to many factors, such as climate change. The test site, constructed in 2008 along Alaska Highway at Beaver Creek, Yukon, Canada, provides valuable information on the long-term thermal response of permafrost underneath transportation infrastructure, to disturbances induced by constructions and climate change. The temperature data collected can also be used to calibrate thermal models to gain insight into relative effects of different factors on the sensitivity of the ground thermal regime underneath transportation infrastructure to on-going climate change. A finite-element, 2D heat conduction model, taking ice-water phase change into account, was developed based on the Beaver Creek experimental site characteristics and conditions. To increase the accuracy of the model, site-specific parameters, such as soil properties, near surface air temperature, and embankment dimension, were measured and used as input parameters. After calibration of the model, sensitivity analysis of certain input parameters, such as air temperature, embankment thickness and ground temperature, was conducted for different site conditions. The model was used to develop an engineering design chart allowing assessing the heat balance at the interface between embankment and natural ground. The heat balance analysis and the design chart are based on the results of sensitivity analysis and validated using the data from the Tasiujaq airstrip in Northern Quebec, Canada.

1. Introduction

Permafrost, defined as one of six cryospheric indicators of global climate change, refers to soil, rock, ice and organic material, with temperatures at or below 0 °C for at least two consecutive years. In the northern hemisphere, about 24% of exposed land area is underlain by permafrost, and about 17% of permafrost area belongs to the discontinuous regions, which are particularly sensitive to climate change (Brown, 1997; Nelson et al., 2002; Zhang et al., 2008).

Physical and mechanical properties of permafrost are highly variable and extremely sensitive to changes in soil temperature. The bearing capacity of permafrost with temperature changing from −4 °C to −1 °C, for example, can decrease to 30% (Cole et al., 1999).

In Alaska, permafrost degradation began in the mid-70s (Osterkamp, 2003), and it has been largely documented in Arctic area (e.g., Lachenbruch and Marshall, 1986; Serreze et al., 2000; Jorgenson et al., 2001; Hinzman et al., 2005; Osterkamp, 2007). Several studies on permafrost vulnerability to climate change were conducted as well (Jorgenson et al., 2001; Lemmen et al., 2008; Grosse et al., 2011; Boyle et al., 2013; Calmels et al., 2015), and they all indicate that permafrost was undergoing severe degradation in response to climate change.

Climate change appears to be a long-term trend, regardless of the success of global initiatives to reduce greenhouse gas emission (Lemmen et al., 2008; Pachauri et al., 2014). The global mean surface temperature between 2081 and 2100, compared to the time period between 1986 and 2005, will increase by 2.6 °C to 4.8 °C, and the warming trend is faster in Arctic area (Pachauri et al., 2014).

According to Canada's 2010 National Communication to the United Nations Convention on Climate Change, the most significant impact of climate change will happen in Arctic areas, and the increase of winter temperature is expected to be larger than that of summer with increasing reaching 8 °C by 2050. Kaplan and New (2006) indicate that climate change has a serious implication for the Arctic, where the temperature will increase at least 1.5 to 2 times as fast as the global temperature. The warming trend will result in increased active layer thickness, reducing the land area underlain by near-surface permafrost and causing extensive ground settlement in ice-rich permafrost regions (Woo et al., 1992; Nelson et al., 2002).

* Corresponding author.
E-mail address: xiangbing.kong.1@ulaval.ca (X. Kong).

https://doi.org/10.1016/j.coldregions.2018.11.013
Received 26 October 2017; Received in revised form 10 August 2018; Accepted 20 November 2018
Available online 22 November 2018
0165-232X/ © 2018 Published by Elsevier B.V.

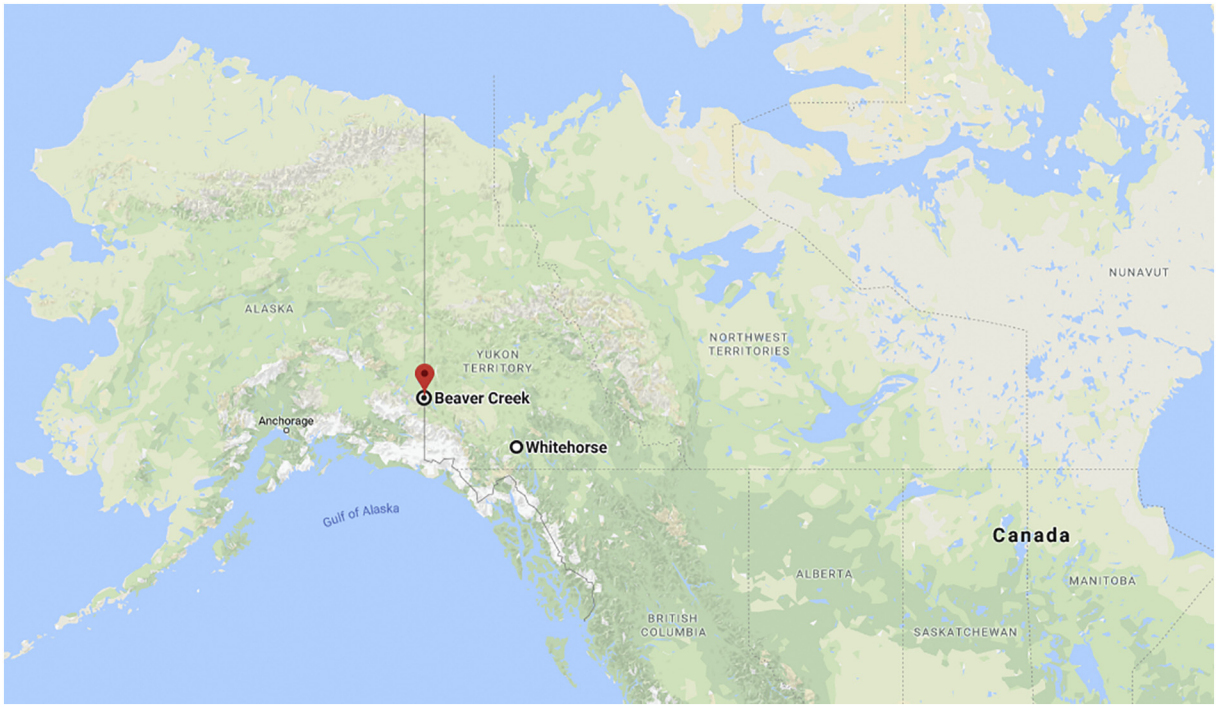

Fig. 1. The location of the Beaver Creek experimental site, along the Alaska Highway, Yukon, Canada. (Source: GoogleEarth.)

The effect of climate change on the civil infrastructure integrity has begun since the second half of the 20th century (Cheng and Wu, 2007; Doré et al., 2016). The processes of climate change, with changes in temperatures, precipitation conditions, wind conditions and the occurrence of extreme weather events, can severely disrupt ecosystems and human transportation infrastructures (Jorgenson et al., 2001), and cause serious consequences to land and air transportation service in permafrost regions (Smith and Levasseur, 2002). Extensive evidence of permafrost engineering failures due to many factors, such as climate change, exists along the Alaska Highway, which passes through extensive areas of warm, ice-rich permafrost (M-Lepage, 2015).

The engineering failures will increase the maintenance cost for the linear-infrastructure in the Arctic region. The estimated additional maintenance cost to maintain roads in permafrost areas, is about $22,000 (CAD) per year per kilometer in Yukon, Canada (Reimchen et al., 2009). Cole et al. (1999) have estimated that about $12 million (USD) are required to maintain the road network in Alaska. Mueller (2007) estimated that the additional cost related to permafrost degradation will exceed $3 million (CAD) per year by 2055 in North-West Territory, Canada.

Although many roads, airports and railways have been designed and constructed in cold regions, little can be found on specific design procedures or guidelines for transportation infrastructure in permafrost conditions. A method based on maintaining the mean annual ground temperature (MAGT) at the base of fill layer below 0 °C was proposed for the design of air convection embankment (Goering, 2002; McHattie and Goering, 2009); however, the permafrost degradation can still happen if a positive thermal gradient exists between MAGT at the base of fill layer and permafrost temperature. Whether permafrost degradation happens or not depends on the total amount of heat flowing into or flowing out of foundation. To maintain permafrost stability under an embankment, the amount of heat flowing out of foundation should be equal or larger than the amount of heat flowing into the foundation during a year. A relatively new approach, based on the measurement of heat flux between the MAGT at interface between the embankment-soil interface and permafrost temperature, is proposed to analyze heat balance through the interface in one year. The proposed method would allow selecting the suitable mitigation techniques based on the quantity of heat to be extracted and the heat extraction capacity of mitigation techniques.

The main objective of this paper is to describe the development of a rational technique to analyze thermal stability of an embankment built over permafrost. More specifically, the paper will include the analysis of the thermal behavior of an embankment in response to climate change, based on the field data in Beaver Creek, Yukon, Canada. It will also include a description of the development of a 2-dimensional heat conduction model, calibrated to the field data from Beaver Creek. The model has then been used to analyze the heat balance through interface with different embankment thickness and site conditions, such as different air temperatures and permafrost temperatures, and to propose an engineering design chart to present the relationship between heat balance and different embankment thicknesses. The engineering design chart has been validated using thermal data from the Tasiujaq airstrip, in Nunavik, Quebec, Canada. The chart is meant to assess permafrost stability under an embankment considering site conditions and to quantify, in unstable cases, the amount of excess heat transferred to permafrost.

2. Study site

To better understand permafrost degradation on linear-infrastructure in permafrost regions, 12 experimental sections with and without mitigation techniques were constructed at the Beaver Creek test site. These mitigation techniques mainly include air convection embankment, longitudinal culvert, heat drain, snow/sun shed, snow clearing technique, grass-covered embankment, insulation and high albedo surface. This test site is located at 62° 20′ N, 140° 50′ W, about 8 km south of the community of Beaver Creek and about 30 km south of the Canada-United States border (Fig. 1). This experimental site is located in an alluvial plain, and has been constructed at km 1865 of the Alaska Highway in 2008. It is located in the extensive discontinuous, warm permafrost region, and the road in this area is experiencing problems related to permafrost thaw.

The climate is cold continental, with long harsh winters and warm

dry short summers (M-Lepage, 2015). Climate records indicated that the mean annual air temperature was about −5.5 °C from 1971 to 2000 (Environment Canada, 2011). Air freezing index and air thawing index are two commonly used climate parameters to quantify the "severity" of winter or summer (Doré and Zubeck, 2009). The average air thawing, freezing index measured at the Beaver Creek weather station between 1971 and 2000 was respectively 1532 °C-day, −3534 °C-day (Environment Canada, 2011).

Mean annual precipitation for the same period is about 419 mm, with 296 mm in the form of water and 123 mm in the form of snow, converted in water equivalent (Environment Canada, 2011). The snowfall begins in September and snowmelt begins in April.

Based on the analysis of soil cores obtained from drilling, four types of soils are present at the site: ice-rich peat with volcanic ash, silt, woody peat and silt, and ice-rich diamicton (M-Lepage, 2015).

3. Ground thermal regime

In this paper, we focus on the reference section. Thermistors strings were installed in 15.5 m deep boreholes in 2008. Thermistors were spaced by a distance of 0.3 m to 1.0 m. Since then, temperatures were measured automatically six times per day, and the data were transmitted by satellite every 4 h to the computer server in Whitehorse, Yukon. The temperature probes, produced by LogTag Recorders Company, have an operating range from −40 °C to 85 °C with a standard recording accuracy of ± 0.1 °C. The thermistor strings were installed under the centerline (BH1), under the center of the side slope (BH2) and in the natural ground at the toe of the slope (BH3). Availability of temperature data collected 6 times per day along three 15.5 m holes across the embankment allows analyzing 2-D temperature variations with time. Fig. 2 illustrates temperatures variations under the centerline of the reference section (BH1) for a four year period from December 2008 to December 2012. The interface between the embankment and the foundation soil is used as the reference level (0 m). From this figure, it can be seen that the embankment thickness of 5.5 m did not prevent the thawing front to penetrate into the natural ground with the thawing depths reaching around 1.0 m underneath the natural ground surface in summer. The 0 °C isotherm reached the interface between embankment and foundation around mid-July.

Another approach proposed to assess thermal stability of permafrost is to quantify the gradient of MAGT as a function of depth in soils

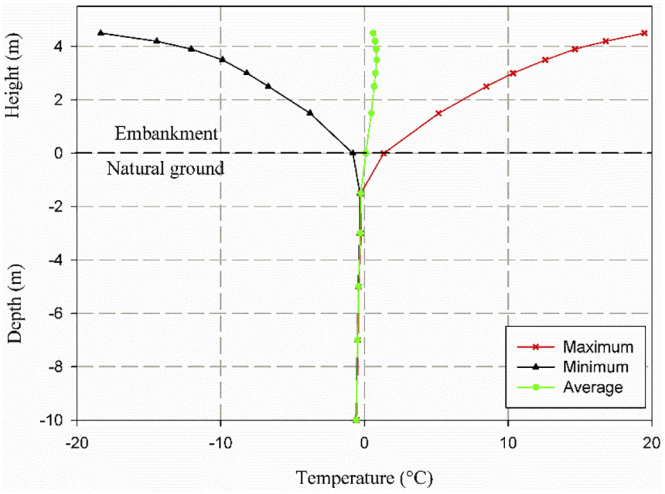

Fig. 3. Mean annual ground temperature (MAGT) envelope under the centerline of the reference section (BH1) in 2010.

(Batenipour et al., 2010). A positive mean annual thermal gradient is an indication of warming and degrading permafrost. Fig. 3 gives an example of a thermal regime for BH1 with a gentle positive thermal gradient showing unstable permafrost conditions.

Fig. 4 illustrates MAGT profiles as a function of depth at the centerline of the reference section during the monitoring period from 2009 to 2012. Fig. 4 shows that the all the mean annual ground thermal gradients in the natural ground were positive, indicating more heat flowing into the permafrost layer from 2009 to 2012. In the embankment, the trend of mean annual temperature variation was irregular with the depth, and the mean annual temperature had the maximum values in 2010, compared to other three years.

The maximum thaw depth is observed around the beginning of November. Figs. 5 and 6 show the temperature profiles with depth in the side slopes (BH2) and at the toe of the embankment (BH3) respectively, on every November 5th during monitoring years 2009 to 2012. Fig. 5 shows that temperature increased in the embankment from 2009 to 2012, with the temperature reaching 1.1 °C and 2.5 °C at the interface in 2009 and 2012, respectively.

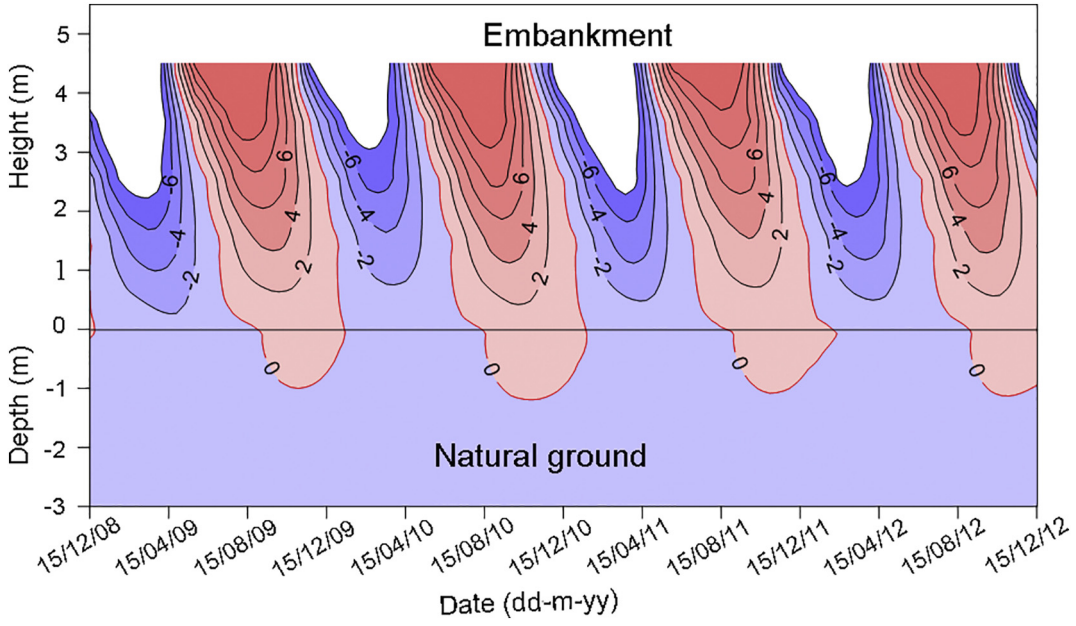

Fig. 2. Thermal behavior of the Beaver Creek experimental embankment under the centerline of the reference section (BH1).

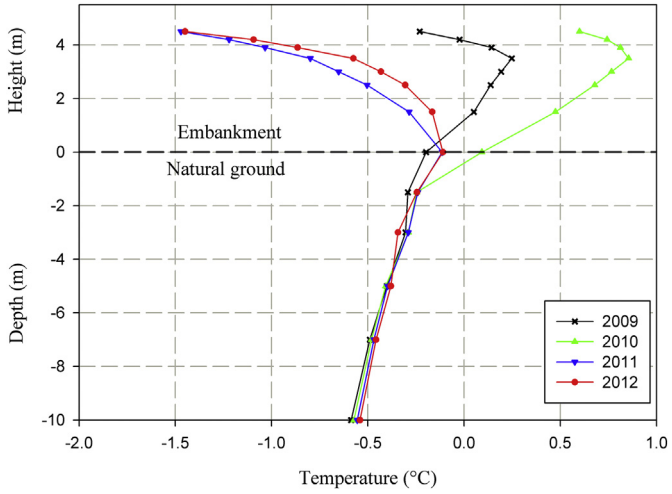

Fig. 4. Mean annual ground temperature (MAGT) profiles with depth under the centerline of the reference section (BH1) from 2009 to 2012.

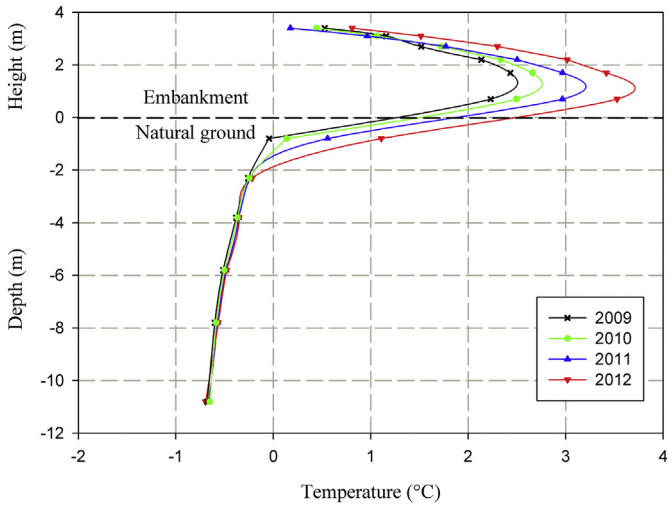

Fig. 5. Temperature profiles on November 5th along the depth in the side slopes of the reference section (BH2) from 2009 to 2012.

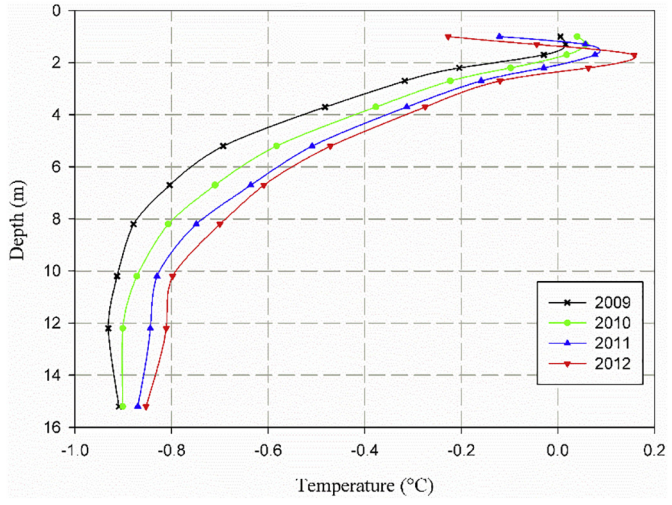

Fig. 6. Temperature profiles on November 5th along the depth at the toe of the reference section (BH3) from 2009 to 2012.

The effect of seasonal air temperature variations decreases with increasing depth in the ground, and from 2009 to 2012, temperatures remained the same 2.3 m below the original ground surface. Fig. 5 shows an increase of the temperatures in the side slopes as well as an increase in thaw depth. The thickness of active layer increased by 1.13 m over the monitoring period, going from 0.75 m to 1.88 m under the interface between the embankment and the foundation soil from 2009 to 2012. The gradual increase of active layer thickness in the side slopes has affected the embankment integrity and, as a result, longitudinal cracks have appeared along embankment edges.

Fig. 6 illustrates the temperature profile in soil at the toe of the embankment slope. It shows that below the first two meters in the natural ground, the temperature increased steadily from 2009 to 2012. The maximum difference of temperature reached 0.22 °C at the depth of 5.2 m below the natural ground surface. The thickness of active layer showed a slight increase as well, going from 1.54 m to 2.38 m from 2009 to 2012.

4. Numerical simulation

A numerical model was built using the SVHeat geothermal modeling software to simulate the case of the reference embankment at the Beaver Creek test site. Actual geometry of embankment and soil properties were used to build the model, which was then calibrated using 4 years of temperature data collected at the site.

4.1. Physics, governing equations and input parameters

The physical domain consists of a normal embankment and foundation soil. The whole domain is used for numerical simulation (Fig. 7), due to the fact that physical domain is not symmetrical.

The physical domain represents an area 44.2 m wide from the centerline of the embankment and a depth of 16.0 m underneath the centerline from road level. In the physical domain, part ① is the embankment fill, which consists of 50% gravel, 30% sand, and 10% silt; part ② is the saturated silt with water content 36% (de Grandpré et al., 2012). Heat conduction is the main heat transfer mode if water flow is not considered in soils, and the equation governing two-dimensional, non-linear heat flow in soils can be expressed as (Newman and Wilson, 1997):

$$\frac{\delta}{\delta x}\left(k_x\frac{\delta T}{\delta x}\right)+\frac{\delta}{\delta y}\left(k_y\frac{\delta T}{\delta y}\right)=C\frac{\delta T}{\delta t}-L_f\frac{\rho_i}{\rho_w}\frac{\delta\theta_i}{\delta} \quad (1)$$

where t is the time (s), T is the temperature (°C), k is the thermal conductivity (J/(s-m-°C)), C is the volumetric heat capacity (J/(m^3-°C)), L_f is the volumetric latent heat of fusion of water, which equals to 3.34×10^8 J/m^3, x, y are coordinates (m). ρ_i, ρ_w are the ice density and water density (kg/m^3), respectively.

In the model, the unfrozen water content in frozen soils varies with soil types and temperature, and the relationship between unfrozen water content and temperature can be expressed as (Tice et al., 1976; Farouki, 1986):

$$\theta_u=\begin{cases}\theta_w & \text{if } T\geq T_f\\ \frac{\rho_d}{\rho_w}a|T|^{-b} & \text{else}\end{cases} \quad (2)$$

where θ_u is the volumetric unfrozen water content (m^3/m^3), θ_w is the volumetric water content of unfrozen soil (m^3/m^3), T_f is the soil freezing point (°C), ρ_d is the soil dry density (kg/m^3), ρ_w is the water density (kg/m^3). a, b are the experimental parameters, whose values are shown in Table 1. An example of unfrozen water content versus temperature using published experimental parameters (Andersland and Ladanyi, 2004) is shown in Fig. 8a.

The unfrozen water content has a large effect on the volumetric heat capacity, C, which is calculated based on the following equation (Farouki, 1986):

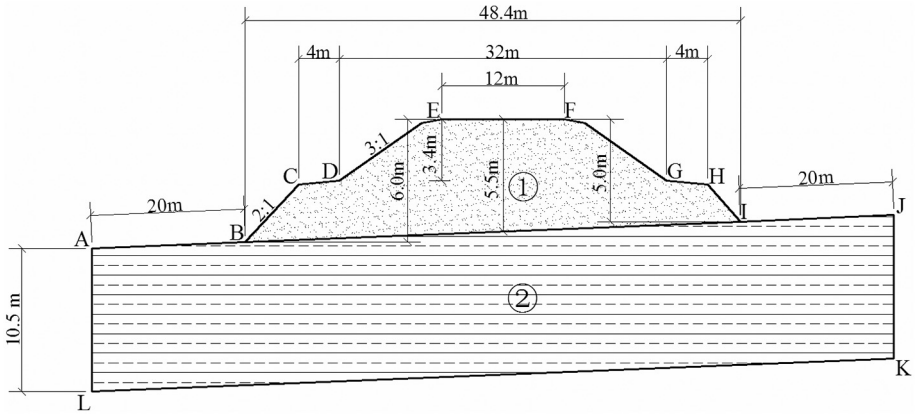

Fig. 7. The physical domain of the embankment and foundation.

Table 1
The values of experimental parameters.

Media	Embankment fill	Silt
a	0.021	0.048
b	0.408	0.326

$$C = \rho_d(c_s + c_w w_u + c_i w_i). \tag{3}$$

where c_s, c_w and c_i are the mass-specific heat of solids, water, and ice, respectively. The values of c_w, c_i are 4184 J/(kg-°C) and 2100 J/(kg-°C), respectively (Farouki, 1986). w_u is the gravimetric unfrozen water content of the soil, and w_i is the gravimetric ice content of the soil.

The measured thermal parameters of foundation soil (silt) from laboratory testing are shown in Table 2 (de Grandpré et al., 2012). The values of thermal conductivity are given in unfrozen state and frozen state with no unfrozen water content varying outside the phase change zone. In this paper, the calculation of thermal conductivity in the phase change zone is done following the method proposed by Johansen (1975). The thermal functions for thermal conductivity and thermal capacity of silt used in this paper are shown in Fig. 8b.

The soil parameters of embankment fill directly affect the temperature distribution in the embankment and, based on laboratory testing, the measured water content of embankment fill in summer varies from 2.3% to 7.2% in different positions of embankment fill (Doré et al., 2007).

The calculation of thermal conductivity, volumetric heat capacity in frozen state and unfroze state for embankment fill, can be estimated using empirical equations for coarse-grained soils (Kersten, 1949):

$$k = \begin{cases} 0.01442 \times (0.7 \log w + 0.4)(10)^{0.6243\rho_d} & \text{if } T \geq T_f \\ 0.01096 \times (10)^{0.8116\rho_d} + 0.00461 \times (10)^{0.9115\rho_d} w & \text{else} \end{cases} \tag{4}$$

$$C = \begin{cases} \left(\frac{\rho_d}{\rho_w}\right)\left(0.17 + 1.0\frac{w_u}{100}\right)C_{vw} & \text{if } T \geq T_f \\ \left(\frac{\rho_d}{\rho_w}\right)\left[\left(0.17 + \frac{1.0w}{100}\right) + 0.5\left(\frac{w\text{-}w_u}{100}\right)\right]C_{vw} & \text{else} \end{cases} \tag{5}$$

where ρ_d is soil dry density (kg/m^3), C_{vw} is volumetric water heat capacity, whose value is 4.187 MJ/(m^3-°C). w is the total gravimetric water content. The subscripts, u and f, mean respectively unfrozen state, and frozen state in soils.

The near-surface temperature is applied on the top boundaries of the physical domain. In general, the approximate sinusoidal curves or cosine curves with a thermal modifier (n-factor) fitting the observed air temperature is often used in numerical simulations. A weather station installed at the site provides detailed information on the air temperature. Air freezing index represents the summation of average daily air temperatures below 0 °C. The air thawing index is the summation of temperatures above 0 °C (Andersland and Ladanyi, 2004). To ensure the accuracy of the thermal simulation, the simulated air freezing and thawing indices should approximate reasonably the indices calculated from measured air temperature. The average calculated field thawing, freezing air index are 1604 °C-day, −3023 °C-day from 2009 to 2013, and the simulated thawing, freezing air index are 1551.5 °C-day, −3025 °C-day. The difference between the calculated and simulated air index is < 4%, and as a result, the simulated air temperature can be used reliably for the simulation (Fig. 9). The n-factor is very sensitive to many factors, such angle of incidence of solar radiation, cloud cover, precipitation and vegetation. On a yearly basis, the freezing n-factor has been observed to vary between 10 and 30% in Yukon Territory (Karunaratne and Burn, 2003). However, to simplify the simulation, constant annual freezing n-factor and annual thawing n-factor are given on the thermal boundaries of numerical models. This assumption involves that the surface conditions, such as vegetation cover, precipitation, wind speed and snow cover, do not vary on a yearly basis.

Constant temperature boundary at the bottom of the model can provide a more efficient computing time, comparing to heat flux boundary (Alfaro et al., 2009). Moreover, considering that the model is not used to assess long-term evolution of permafrost temperature, a fixed temperature condition can thus be applied at the bottom of the model. The measured permafrost temperature of −0.56 °C is therefore applied along the boundary KL. The near-surface temperatures with a modifier (n-factor) are applied on the top boundaries of the physical domain (ABCDE and FGHIJ), and the lateral boundaries (AL and JK) are assumed to be adiabatic.

4.2. Models calibration

The computational domain, shown in Fig. 7, was divided into 3104 nodes and 1473 triangular finite elements, with a greater element density in the embankment fill and natural ground surface layer underneath the embankment to obtain a better solution for the active layer and the top part of permafrost.

A detailed calibration procedure was carried out using 4 years of temperature data to try to reproduce the ground thermal regime underneath the embankment. Table 3 is the summary of the iterations that were done to calibrate the model. Based on the field temperature data, the ground thermal regime changed from 2009 to 2013 due to many factors, such as the variation of air temperature, wind speed, relative humidity and precipitations. In order to average the variation of contributing factors on the ground thermal regime, the average 4-years record of temperature distribution was selected as the reference to calibrate the model.

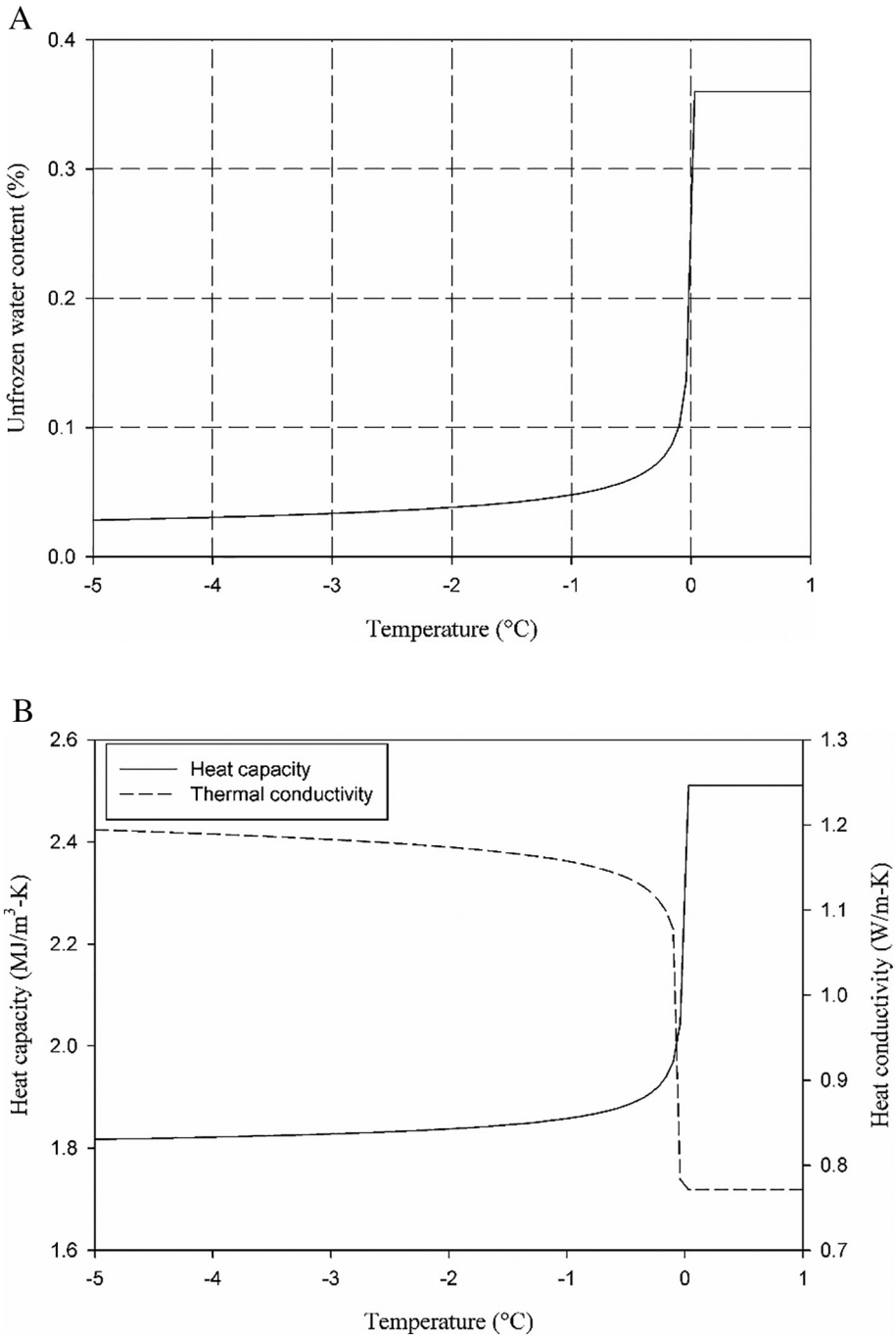

Fig. 8. Thermal functions used in the model: (a) unfrozen water content versus temperature for silt; (b) thermal conductivity and heat capacity for silt (Johansen, 1975).

Table 2
Physical parameters measured in the foundation soil at Beaver Creek (de Grandpré et al., 2012).

Physical variable	k_f (W/m-K)	k_u (W/m-K)	C_f (MJ/m^3-K)	C_u (MJ/m^3-K)	θ (m^3/m^3)	S_r (%)
Silt	1.21	0.76	1.73	2.51	0.36	100

The simulated sinusoidal air temperature (Fig. 9), measured embankment dimension (Fig. 7) and measured soil parameters (Table 2), were used in the model iterations. In the following discussion, each experimental model iteration was labeled with "I". The validation process began with I1 and ended in I2c. The first step in the modeling was to determine the initial ground temperatures, which were applied in the following transient steps. I1 represented the steady state analysis, which was used to generate the initial ground temperature for the next analysis. In I1, the temperature boundaries for steady state analysis were obtained from the monitored ground temperature at different depths.

One thing to note is that the measured unfrozen thermal conductivity is about 1.40 J/(s-m-°C) in the shallow part of the embankment fill, and the thermal conductivity should be consistent with this value to react to the field thermal parameters. Through the above eq. (4), the water content 3% and density 1800 kg/m^3 were assigned for the whole embankment fill in the initial model iteration in I1.

I2 was built upon I1, and all the model iterations were 25 year-long

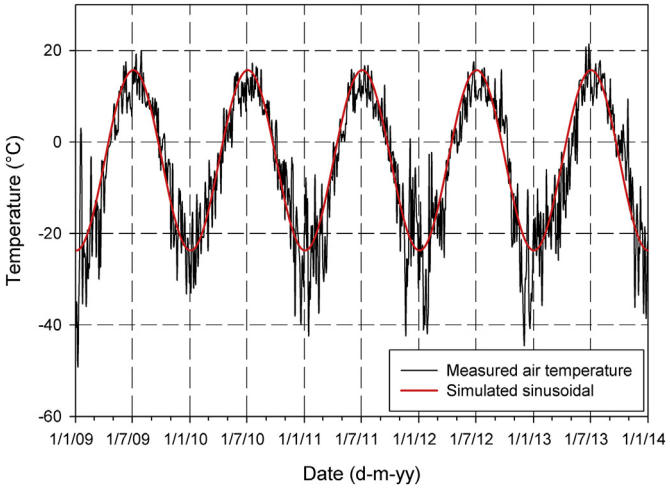

Fig. 9. Graphical comparison between measured air temperature and simulated sinusoidal temperature.

to obtain a stable annual cycle, which responded to the given thermal boundaries and material properties of soils. The time of model iterations was 5 years longer than that used in the previous models (Buteau et al., 2004).

The model was ran, using automatic time steps chosen by the finite element software in the first 20 years to save time and to avoid numerical crashing, and after the 20 years period, time step was set to 1.0 day, with results saved every day. The numerical results for the final year for all the following model iterations were exported for the future temperature analysis.

Air temperature and n-factor are the most critical driving input parameters for the ground thermal regime, comparing to other parameters, such as the thermal properties of foundation soil (Darrow, 2011). The n-factor used in I2 are given in Table 4. I2a, was similar to I2, except that the embankment surface n-factor was adjusted to improve the quality of the fit between the modeled and observed ground temperature regime. Through sensitivity analysis, the adjusted embankment surface thawing (n_t), freezing n-factor (n_f) are 1.4 and 1.0, respectively. Snow depth and density strongly affect ground temperature (e.g., Jorgenson et al., 2001). The temperature at the base of the embankment and in subgrade soils is controlled by embankment surface boundary and side slopes boundary conditions. I2b was built on I2a, adjusting the n_t, n_f on the side slopes through sensitivity analysis. The n_t, n_f in the side slopes obtained from the analysis were 1.2, and 0.97, respectively. The values of n_t and n_f chosen for different thermal boundaries are given in Table 5.

MAGT profile with depth is a good indication of heat flow direction across the interface between embankment and subgrade soil in one year (Batenipour et al., 2010). It is also a good indicator for model fit to measured temperature data.

Mean annual vertical temperature profiles under the centerline of the embankment generated using the three models described above are shown in Fig. 10. The average temperature profile measured at the site is also shown in the figure for comparison. For I2, comparison between the modeled temperatures and the measured field temperatures as a function of depth indicates that temperature discrepancy decreases with depth. In addition, the modeled temperatures are typically 0.04 °C to 0.75 °C warmer than the measured temperature in the subgrade soil.

With the adjusted n-factor on the embankment surface in I2a, a significant difference of temperatures still existed in the 4 m below embankment surface. However, soil temperatures in the natural ground are closer to the measured temperatures, typically within 0.2 °C of the measured average temperature below the interface, with the biggest temperature difference at the interface between embankment and subgrade soil. For I2b, the modeled temperatures matched the measured temperatures within 0.06 °C in the subgrade soil. The results for I2c, were similar to I2b, with a better fit in the embankment fill, close to the interface. The measured water content ranges from 2.3% to 7.2% in

Table 4
N-factor used in I2.

Surface type	n_t	n_f
Natural ground surface	0.5	0.5
Embankment surface	1.8	1.0
Embankment side slopes	1.1	0.5

Values obtained from literature (Goering, 2003; Andersland and Ladanyi, 2004; Zottola et al., 2012).

Table 5
Final determined n-factor for different thermal boundaries.

Surface type	n_t	n_f
Natural ground surface	0.50[a]	0.50[a]
Embankment surface	1.4[b]	1.0[b]
Embankment side slopes	1.2[b]	0.97[b]

[a] Values obtained from the literature (Goering, 2003; Zottola et al., 2012).
[b] Values obtained through sensitivity analysis.

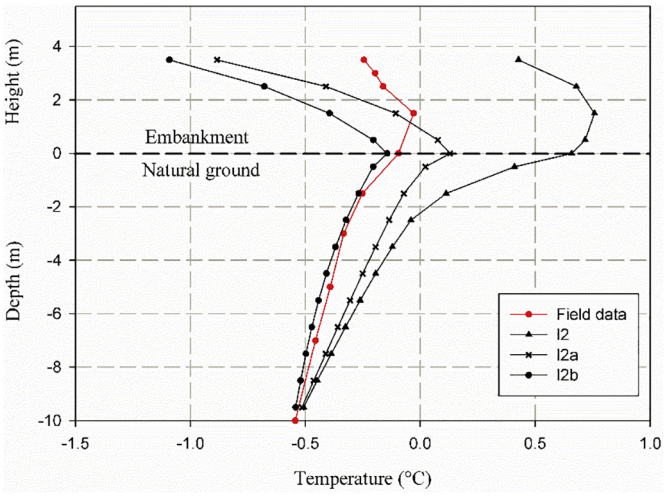

Fig. 10. Comparison of 4-year average temperature profiles with depth at the centerline of the embankment measured at the site and obtained with simulations I2, I2a, and I2b.

Table 3
Summary of model iterations.

Iteration	Comments
I1	Steady-state analysis for the initial temperature regime, based on field data
I2	Initial model iterations: simulated over a 25-year period model with thawing, freezing n-factor from literature for different thermal boundaries.
I2a	Revise I2 using adjusted n-factor for embankment surface to make the MAGT along the centerline in the embankment, close to measured field data
I2b	Revise I2a using adjusted n-factor in the side slopes to make the MAGT at the interface close to field data
I2c	Revise I2b, and add a layer (0.5 m thickness) with higher water content above the interface to improve accuracy

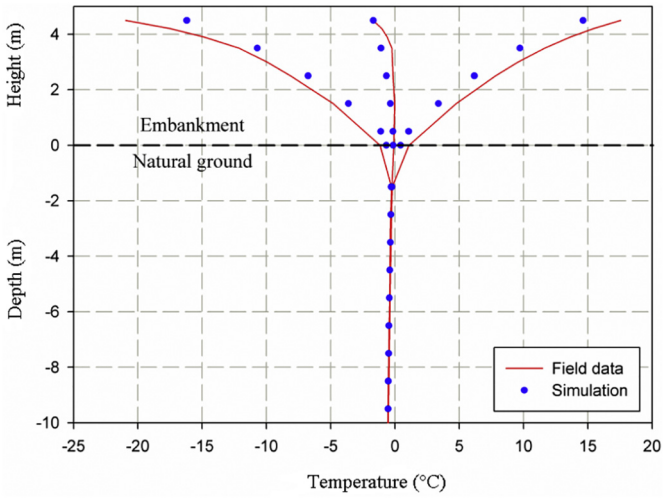

Fig. 11. Comparison of maximum, minimum and average temperature profiles with depth at the centerline between field data and numerical simulation I2c.

embankment fill, and in I2c, a 0.5-m thick layer of embankment with a higher water content was specified at the bottom of the embankment improving the accuracy of the simulation. The final calibrated results of I2c simulation including maximum, minimum and average temperature profiles at the centerline is shown in Fig. 11.

The results indicate that the modeled average temperature was typically 0.05 °C to 0.85 °C colder than the measured temperature in the embankment. Below the embankment-soil interface, the modeled temperature fitted the measured temperature well, and the maximum temperature difference was < 0.1 °C. Comparison between the modeled maximum temperature with the measured maximum temperature indicates that the temperature difference decreased with the depth in the embankment with the temperature difference of 0.66 °C occurring at the embankment-soil interface. Below the embankment-soil interface, the maximum temperature difference was < 0.1 °C. For the minimum temperature, the modeled temperature was warmer than the measured temperature in the embankment, and the difference was 0.48 °C at the embankment-soil interface.

5. Analysis, validation and discussion

Heat balance is the summation of all negative and positive heat fluxes passing through a plane during a year. M-Lepage et al. (2012) have proposed the use of two indices, the induction index, and extraction index, to quantify heat balance at the interface between an embankment and subgrade soils. Heat balance equals to induction index plus extraction index, which are expressed as:

$$H_x = k_{frozen} \times \frac{T_1 - T_2}{\Delta z} \times \Delta t \quad (6)$$

$$H_i = k_{unfrozen} \times \frac{T_1 - T_2}{\Delta z} \times \Delta t \quad (7)$$

where H_x, H_i are the extraction index and induction index, respectively. T_1, T_2 are the ground temperatures at depth of h_1, h_2 under the interface. Δz is the absolute difference between $h_1$and h_2. k_{frozen}, $k_{unfrozen}$ are the thermal conductivity at frozen and thawing states in the surface ground layer. In this paper, Δz, Δt are specified to be 10.5 m and 1.0 day, respectively.

After the model was calibrated by the measured field temperature data at Beaver Creek, sensitivity analyses were carried out to quantify heat balance through the soil-embankment interface at the centerline for different embankment thicknesses and site conditions. The analysis was done with the model calibrated using 4 years of data collected at the test site and is considered to be representative of thermal conditions for those 4 years. Thus, it does not consider the effect of long-term climate change at the top thermal boundaries of models.

In the sensitivity analysis, the permafrost temperature was set at −1 °C and different values of mean annual air temperature and embankment thickness were used to obtain different thermal gradients between the interface and bottom boundary to simulate the different thermal conditions for different embankment thicknesses and site conditions. Thermal gradients were calculated based on the MAGT at the interface and constant bottom temperature in the model.

To obtain the constant thermal gradient between the interface and bottom boundary, a time length for every sensitivity analysis was set to be 60 years. MAGT was plotted as function of time and when temperature became stable, the full temperature variation in that year was used for the sensitivity analysis. The relationships between heat balance through interface and embankment thickness, thermal gradient, were obtained through statistical regression (Table 6) using data points obtained by numerical simulation. The results of the quantification of heat balance through the embankment-soil interface at the centerline of the embankment for different embankment thicknesses and air temperatures are shown in Fig. 12. From the figure, it can be seen that heat balance increases with thermal gradient for all embankment thickness and nonlinearity is obvious for the thicker embankments. For example, with a thermal gradient of 0.1 °C/m, the corresponding heat balances were -2.4×10^6 J/m^2, 1.0×10^6 J/m^2, 2.5×10^6 J/m^2, 3.1×10^6 J/m^2 for embankment thickness 1.0 m, 2.5 m, 4.0 m and 5.5 m, respectively. Increasing embankment thickness is considered as an effective method to protect permafrost by improving thermal resistance. However, for thicknesses > 4.0 m, the effectiveness of this method decreases significantly.

The model was calibrated using observed maximum, minimum and average temperature profiles with depth at the centerline of the embankment. However, the temperature profiles did not include the detailed information on temperature changes with time in 1 year, which was required to calculate heat balance through the interface. The calculated mean annual heat balance based on field data over the period from 2009 to 2013, was 1.1 MJ/m^2 and the value obtained from Fig. 12 was around 1.4 MJ/m^2. The difference of 0.3 MJ/m^2 between the modeled results and the measured heat balance can be attributed to the fact that the measured temperature along the centerline at the interface had a larger range varying between −1.16 °C and 1.09 °C, while the modeled temperature range was between −0.68 °C and 0.43 °C. For each embankment thickness, the critical thermal gradient corresponding to zero heat balance through the interface can be obtained from Fig. 12. As shown in Fig. 13, critical thermal gradient are generally above 0 °C/m and vary between 0.175 °C/m and −0.003 °C/m

Table 6
Regression equations between heat balance at the embankment-soil interface, embankment thickness and thermal gradient.

Embankment thickness (m)	Regression equation	Coefficient of determination (R^2)
1.0	$Q = 3.06 \times 10^7 \times x - 5.34 \times 10^6$	> 0.99
2.5	$Q = 3.17 \times 10^7 \times x - 2.22 \times 10^6$	> 0.99
4.0	$Q = -0.55 \times 10^6 + 3.31 \times 10^7 \times x - 2.56 \times 10^7 \times x^2$	> 0.99
5.5	$Q = 0.028 \times 10^6 + 3.42 \times 10^7 \times x - 3.81 \times 10^7 \times x^2$	> 0.99

x is the thermal gradient (°C/m) between the MAGT at interface and permafrost temperature; Q is the heat balance (J/m^2) through the interface.

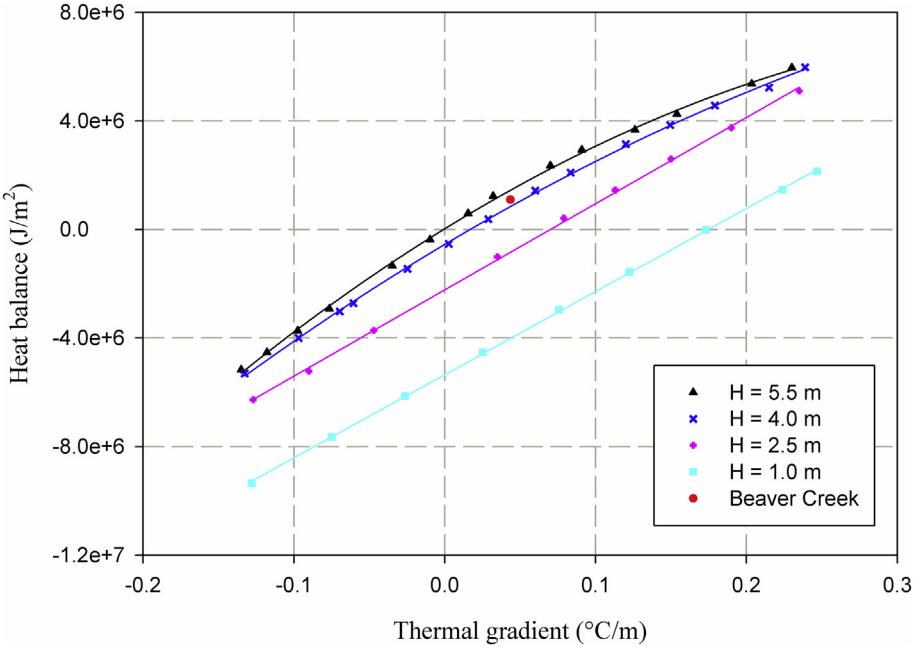

Fig. 12. Heat balance at the embankment-soil interface as a function of embankment thickness (H) and thermal gradient.

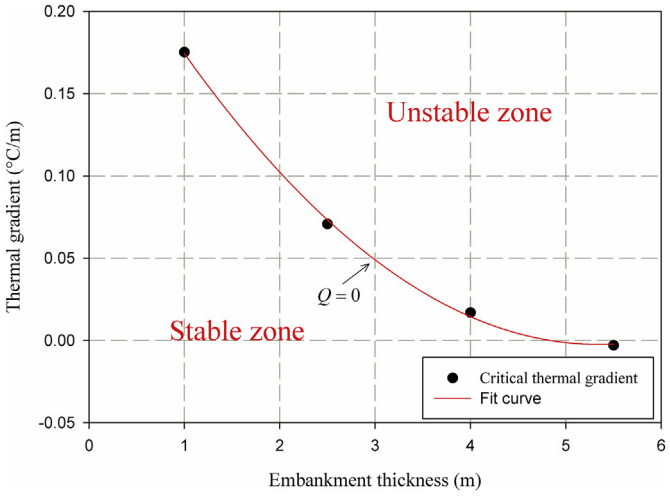

Fig. 13. Critical thermal gradient as a function of embankment thickness.

for different embankment thicknesses. The critical thermal gradient decreases with embankment thickness following a non-linear relationship. Above the critical thermal gradient, heat balance is positive, which means permafrost underneath transportation infrastructure is undergoing degradation and is unstable.

Engineers pay much attention to the thermal state of permafrost underneath transportation infrastructure, and Fig. 13 can help make a preliminary assessment based on measured or estimated temperature underneath transportation infrastructure.

The proposed engineering design chart has been developed based on the model built and calibrated using data from the Beaver Creek test site. It needs to be validated using data from other field sites to improve its reliability. Additional validation data was obtained from the Tasiujaq airstrip in Nunavik, Quebec, Canada. The construction of the airstrip in Tasiujaq was completed in 1990 and the site is located in a extensive discontinuous permafrost zone. The permafrost underneath the airport is ice-rich and thaw-sensitive. Differential settlements had been observed along the length of the runway (Doré et al., 2007). The thickness of the embankment at the location of the instrumentation is 2.45 m and the subgrade soils underneath embankment are medium coarse sand (0–1.45 m) overlying ice-rich silty sand (1.45 m–5.20 m), coarse sand and gravel (5.20 m–9.70 m) and silty clay (9.70 m–27 m) (Allard et al., 2009). Two thermistor cables were installed at the centerline of the runway, at 5.4 m and 13.5 m depth.

The temperature data at the interface and permafrost temperature at the depth of 13.5 m, available on a daily basis, were used to calculate the thermal gradient and associated heat balance through the interface. In Eqs. (6) and (7), heat balance highly depends on the frozen and unfrozen soil conductivities. For a different type of soils, the heat balance chart cannot be used directly. It can, however, be corrected by multiplying the heat balance by the ratio between thermal conductivity of the new soil and of the soil used in the model. The heat balance, at Tasiujaq, has been calculated and is plotted into the engineering design chart for the period going from 2011 to 2014 as shown in Fig. 14. The results indicate that the annual heat balance is in good agreement with the heat balance curve for an embankment thickness of 2.5 m.

Also, the averaged and annual heat balances from 2011 to 2014 are negative, which suggest permafrost degradation underneath embankment did not happen from 2011 to 2014. This is confirmed by the decreasing active layer thickness from 2011 to 2014 (Fig. 15) and by decreasing temperature at the depth of 9.0 m below embankment surface at the centerline from 2011 to 2014 (Fig. 16).

In summary, the engineering design chart has been successfully validated by the calculated heat balance using temperature data from the Tasiujaq airstrip. The design chart should be used with caution when applied to different soils. Heat balance can be corrected by multiplying the ratio between thermal conductivity of subgrade soils at the site considered and of the soil used in the development of the model.

Climate warming will lead to the warming of soils, and the warming rate of soils decrease with depth underneath the natural ground surface. As a result, the mean annual thermal gradient between the embankment-soil interface temperature and permafrost temperature is likely to increase for a given site depending on site conditions and embankment thickness. Based on the expected change of the mean annual thermal gradient and using Fig. 12, it is possible to assess the amount of extra heat flowing into the subgrade soil due to climate warming and to estimate when the embankment is likely to become unstable based on the characteristic of the changing thermal gradient and a selected scenario

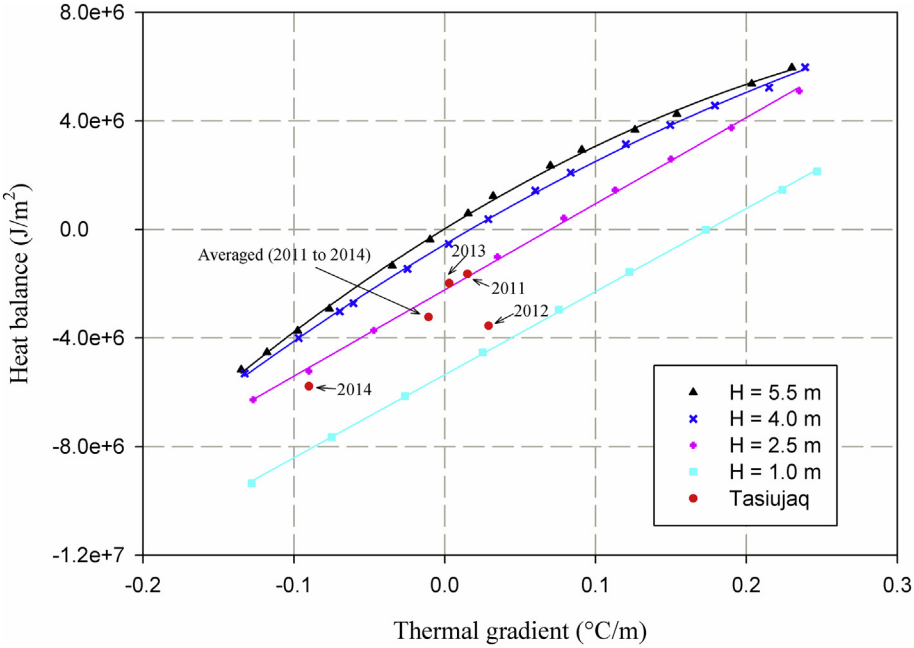

Fig. 14. Validation of heat balance using Tasiujaq airstrip temperature data.

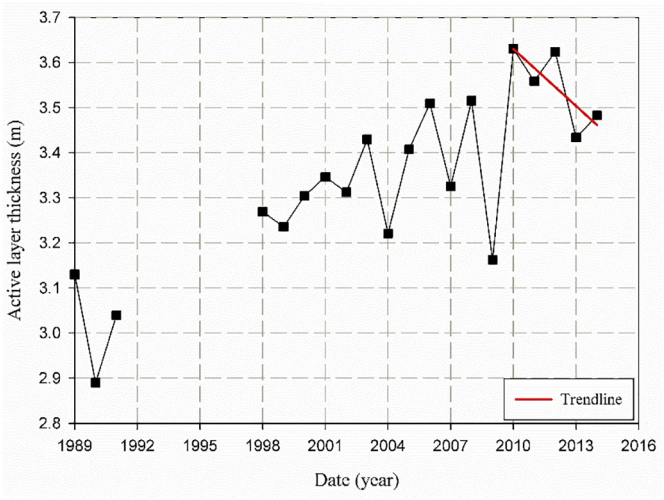

Fig. 15. Evolution of the active layer thickness with time at the centerline of Tasiujaq airstrip.

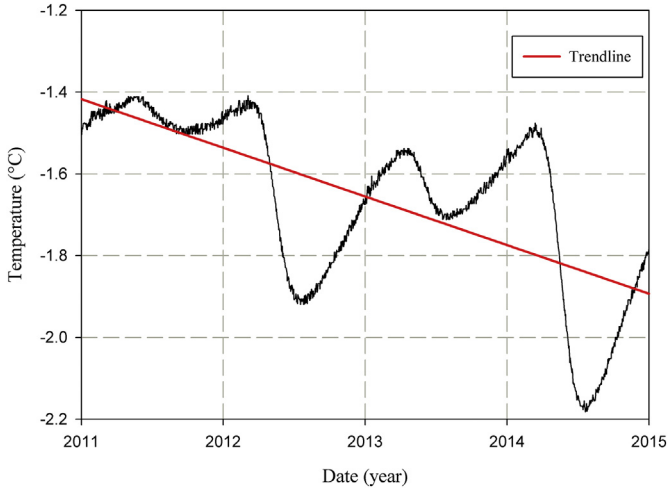

Fig. 16. Evolution of ground temperature at the depth of 9.0 m below embankment surface at the centerline of Tasiujaq airstrip.

of climate warming at the site.

6. Conclusion

The beaver Creek test site, built along Alaska Highway at Beaver Creek, Yukon, Canada, provided valuable information on the long-term thermal response of permafrost underneath transportation infrastructure in the northern regions. In response to both disturbance induced by constructions and climate change, the increase in ground temperature and active layer thickness were observed at this field site.

A 2D, thermal conduction model, taking ice-water phase change into account, was developed and calibrated using the monitored field data from the reference section of the test site. To increase the accuracy of the model, site-specific parameters, such as soil properties, near surface air temperature, and embankment dimension, were measured and used as input parameters into the 2D model. A detailed calibration procedure was proposed, and the final numerical results over the period of 25 years were in a good agreement with temperature data monitored at Beaver Creek, although neglecting the complex effect of uneven snow accumulation on the side slopes in the model.

A relatively new method based on the calculation of heat balance at the embankment-soil interface, has been used in this study. The proposed method allows to determine if permafrost degradation underneath transportation infrastructure is happening or will happen, based on a given site conditions and embankment thickness. An engineering design chart, to estimate heat balance at the embankment-soil interface, was developed based on the calibrated model and has been successfully validated using the data from the Tasiujaq airstrip, in Nunavik, Quebec, Canada. The numerical results indicated that for all embankment thicknesses considered, the relationships between heat balance and thermal gradient have similar trends with heat balance increasing with thermal gradients, and embankment thickness. For the same thermal gradient, the increase in embankment thickness has much more effect on heat balance for thin embankments than for thick embankments. For each embankment thickness, one critical thermal gradient corresponding to zero heat balance can be obtained from the design chart.

Above the critical thermal gradient, the embankment is thermally unstable and permafrost degradation is likely to occur. The critical thermal gradient decreases with increasing embankment thickness following a non-linear trend.

The effect of climate warming can be integrated into the proposed procedure by increasing the mean annual thermal gradient between the embankment-soil interface and permafrost considering a climate change scenario selected by the designer. The expected change in air temperature can be used to estimate the change in average yearly temperature at the embankment-soil interface and consequently, the change in temperature gradient. It would thus be possible to predict the time when permafrost underneath transportation infrastructure is likely to become unstable, if currently stable.

The numerical results were obtained based on the heat conduction model. For future work involving numerical modeling, it is suggested to 1) consider the effect of possible water flow in the active layer on heat balance at the embankment-soil; 2) calibrate thermal models, by comparing the modeled ground temperatures with observed ground temperature and by comparing heat balance with active layer thickness evolution and temperature data history at selected depths.

Acknowledgements

The authors would like to acknowledge the financial support of the Natural Sciences and Engineering Research Council of Canada as well as the technical and financial support of public and private partners of the permafrost engineering research program ARQULUK for this project. The contribution of the Center for Northern Studies of Laval University, who provided data for model validation, is also gratefully acknowledged.

References

Alfaro, M.C., Ciro, G.A., Thiessen, K.J., Ng, T., 2009. Case study of degrading permafrost beneath a road embankment. J. Cold Reg. Eng. 23 (3), 93–111.

Allard, M., Doré, G., L'Hérault, E., Sarrazin, D., Verreault, J., 2009. Investigations géotechniques, caractérisation du pergélisol et stratégie d'adaptation pour les aéroports du MTQ au Nunavik. In: Rapport d'étape. Vol. 2. Centre d'études Nordiques, Université Laval, Quebec, Canada, pp. 1–83.

Andersland, O.B., Ladanyi, B., 2004. Frozen ground engineering. John Wiley & Sons.

Batenipour, H., Kurz, D., Alfaro, M., Graham, J., Kalynuk, K., 2010. Results from an instrumented highway embankment on degraded permafrost. In: Proceedings of the 63rd Canadian Geotechnical Conference & 6th Canadian Permafrost Conference. Calgary, Alberta, Canada, pp. 512–519.

Boyle, J., Cunningham, M., Dekens, J., 2013. Climate Change Adaptation and Canadian Infrastructure. International Institute for Sustainable Development (IISD), Winnipeg, Manitoba, Canada, pp. 1–40.

Brown, J. (1997). Disturbance and recovery of permafrost terrain. Disturbance and Recovery in Arctic Lands: An Ecological Perspective, 167–178.

Buteau, S., Fortier, R., Delisle, G., Allard, M., 2004. Numerical simulation of the impacts of climate warming on a permafrost mound. Permafr. Periglac. Process. 15 (1), 41–57.

Calmels, F., Roy, L., Laurent, C., Pelletier, M., Kinnear, L., Benkert, B., Horton, B., Pumple, J., 2015. Vulnerability of the North Alaska Highway to Permafrost Thaw: A Field Guide and Data Synthesis. Northern Climate ExChange, Yukon Research Centre. Yukon College, Canada, pp. 1–120.

Cheng, G., Wu, T., 2007. Responses of permafrost to climate change and their environmental significance, Qinghai-Tibet Plateau. J. Geophys. Res.: Earth Surface 112 (F2).

Cole, H., Colonell, V., Esch, D., 1999. The economic impact and consequences of global climate change on Alaska's infrastructure: assessing the consequences of climate change for Alaska and the Bering sea region. In: Workshop Proceedings Summarized for the US Global Change Research Program. University of Alaska Fairbanks, USA, pp. 43–56.

Darrow, M.M., 2011. Thermal modeling of roadway embankments over permafrost. Cold Reg. Sci. Technol. 65 (3), 474–487.

Doré, G., Niu, F., Brooks, H., 2016. Adaptation methods for transportation infrastructure built on degrading permafrost. Permafr. Periglac. Process. 27 (4), 352–364.

Doré, G., Pierre, P., Juneau, S., Lemelin, J., 2007. Expérimentation de méthodes de mitigation des effets de la fonte du pergélisol sur les infrastructures du Nunavik: aéroport de Tasiujaq, Rapport d'étape 1–Compte rendu des travaux d'instrumentation et de supervision de construction des planches expérimentales de l'aéroport de Tasiujaq, description des planches construites et de l'instrumentation installée. GRINCH, Université Laval, Quebec, Canada.

Doré, G., Zubeck, H.K., 2009. Cold regions Pavement Engineering. McGraw-Hill, New York.

Environment Canada, 2011. Canadian Climate Normals 1971–2000 [Online]. Available from. http://www.climat.meteo.gc.ca (accessed on July 4 2011).

Farouki, O.T., 1986. Thermal properties of soils. In: seres of Rock and Soil Mechanics. 11. Trans. Tech. Publ., Clausthal-Zellerfeld, Germany, pp. 1–136.

Goering, D.J., 2002. Convective cooling in open rock embankments. In: Proceedings of the 11th International Conference on Cold Regions Engineering, Anchorage, Alaska, USA, pp. 629–644.

Goering, D., 2003. Passively cooled railway embankments for use in permafrost areas. J. Cold Reg. Eng. 17 (3), 119–133.

de Grandpré, I., Fortier, D., Stephani, E., 2012. Degradation of permafrost beneath a road embankment enhanced by heat advected in groundwater 1. Can. J. Earth Sci. 49 (8), 953–962.

Grosse, G., Romanovsky, V., Jorgenson, T., Anthony, K.W., Brown, J., Overduin, P.P., 2011. Vulnerability and feedbacks of permafrost to climate change. Eos, Trans. Am. Geophys. Union 92 (9), 73–74.

Hinzman, L.D., Bettez, N.D., Bolton, W.R., Chapin, F.S., Dyurgerov, M.B., Fastie, C.L., Griffith, B., Hollister, R.D., Hope, A., Huntington, H.P., 2005. Evidence and implications of recent climate change in northern Alaska and other arctic regions. Clim. Chang. 72 (3), 251–298.

Johansen, Ø., 1975. Thermal conductivity of soils. Ph.D thesis, University of Trondheim. (in Norwegian). Translated in U.S. Army, Cold Regions Research and Engineering Laboratory, Translation 637.

Jorgenson, M.T., Racine, C.H., Walters, J.C., Osterkamp, T.E., 2001. Permafrost degradation and ecological changes associated with a warmingclimate in Central Alaska. Clim. Chang. 48 (4), 551–579.

Kaplan, J.O., New, M., 2006. Arctic climate change with a 2°C global warming: timing, climate patterns and vegetation change. Clim. Chang. 79 (3–4), 213–241.

Karunaratne, K., Burn, C., 2003. Freezing n-factors in discontinuous permafrost terrain, Takhini river, Yukon Territory, Canada. In: Proceedings of the 8th International Conference on Permafrost, pp. 519–524 University of Zurich, Switzerland.

Kersten, M.S., 1949. Laboratory research for the determination of the thermal properties of soils. Research Laboratory Investigations, Engineering Experiment Station, University of Minnesota, Minneapolis. Technical Report 23.

Lachenbruch, A.H., Marshall, B.V., 1986. Changing climate: geothermal evidence from permafrost in the Alaskan Arctic. Science 234, 689–697.

Lemmen, D.S., Warren, F.J., Lacroix, J., Bush, E., 2008. From Impacts to Adaptation: Canada in a Changing Climate. Government of Canada, Ottawa, Canada, pp. 448.

McHattie, R.L., Goering, D.J., 2009. Air convection embankment (ACE) design guide. Alaska. Department of Transportation. Report, FHWA-AK-RD-09-06.

M-Lepage, J., 2015. Experimentation of mitigation techniques to reduce the effects of permafrost degradation on transportation infrastructures at Beaver Creek experimental road site (Alaska Highway, Yukon). Mater's thesis, Laval University, Quebec, Canada.

M-Lepage, J., Doré, G., Fortier, D., Murchison, P., 2012. Thermal performance of the permafrost protection techniques at Beaver Creek experimental road site, Yukon, Canada. In: Proceedings of the 10th International Conference on Permafrost, Salekhard, Russia, pp. 261.

Mueller, B., 2007. Climate Change and Transportation in the NWT. Department of Transportation-Planning, Government of the NWT 06–6855-5000. pp. 1–96.

Nelson, F.E., Anisimov, O.A., Shiklomanov, N.I., 2002. Climate change and hazard zonation in the circum-Arctic permafrost regions. Nat. Hazards 26 (3), 203–225.

Newman, G.P., Wilson, G.W., 1997. Heat and mass transfer in unsaturated soils during freezing. Can. Geotech. J. 34 (1), 63–70.

Osterkamp, T., 2003. A thermal history of permafrost in Alaska. In: Proceedings of the 8th International Conference on Permafrost, University of Zurich, Switzerland, pp. 863–868.

Osterkamp, T., 2007. Characteristics of the recent warming of permafrost in Alaska. J. Geophys. Res.: Earth Surface (F2), 112.

Pachauri, R.K., Allen, M.R., Barros, V.R., Broome, J., Cramer, W., Christ, R., Church, J.A., Clarke, L., Dahe, Q., Dasgupta, P., 2014. Climate Change 2014: Synthesis Report. Contribution of Working Groups I, II and III to the Fifth Assessment Report. Intergovernmental Panel on Climate Change IPCC, Geneva, Switzerland, pp. 151.

Reimchen, D., Doré, G., Fortier, D., Walsh, R., 2009. Cost and constructability of permafrost test sections along the Alaska Highway, Yukon. In: Proceedings of the Transport Association of Canada Annual Conference. Vancouver, B.C, Canada, pp. 1–20.

Serreze, M., Walsh, J., Chapin, F.S., Osterkamp, T., Dyurgerov, M., Romanovsky, V., Oechel, W.C., Morison, J., Zhang, T., Barry, R., 2000. Observational evidence of recent change in the northern high-latitude environment. Clim. Chang. 46 (1–2), 159–207.

Smith, O.P., Levasseur, G., 2002. Impacts of Climate Change on Transportation Infrastructure in Alaska. The Potential Impacts of Climate Change on Transportation. pp. 151–160.

Tice, A.R., Anderson, D.M., Banin, A., 1976. The Prediction of Unfrozen Water Contents in Frozen Soils from Liquid Limit Determinations. U.S. Army Cold Regions Research and Engineering Laboratory. CRREL, Report 76–8.

Woo, M.-k., Lewkowicz, A.G., Rouse, W.R., 1992. Response of the Canadian permafrost environment to climatic change. Phys. Geogr. 13 (4), 287–317.

Zhang, T., Barry, R., Knowles, K., Heginbottom, J., Brown, J., 2008. Statistics and characteristics of permafrost and ground-ice distribution in the Northern Hemisphere. Polar Geogr. 31 (1–2), 47–68.

Zottola, J., Darrow, M., Daanen, R., Fortier, D., de Grandpré, I., 2012. Investigating the Effects of Groundwater Flow on the Thermal Stability of Embankments over Permafrost. Cold Regions Engineering 2012: Sustainable Infrastructure Development in a Changing Cold Environment. pp. 601–611.